

Supporting information for the manuscript

A Unique Silk Mat-Like Structured Pd/CeO₂ as an Efficient, Visible Light Photocatalyst for Green Organic Transformation in Water

Yanhui Zhang,^{†,‡} Nan Zhang,^{†,‡} Zi-Rong Tang,[‡] and Yi-Jun Xu^{†,‡,*}

[†] *State Key Laboratory Breeding Base of Photocatalysis, College of Chemistry and Chemical Engineering, Fuzhou University, Fuzhou, 350002, P. R. China*

[‡] *College of Chemistry and Chemical Engineering, New Campus, Fuzhou University, Fuzhou, 350108, P. R. China*

**To whom correspondence should be addressed. Tel./fax: +86 591 83779326*

E-mail Address: yjxu@fzu.edu.cn

Contents List:

Figure S1. Typical TEM images of Pd/commercial CeO₂.

Figure S2. Typical SEM image of Pd/commercial CeO₂.

Figure S3. Controlled experiments using the bare CeO₂ nanoparticles (CeO₂-NPs) and commercial CeO₂ for oxidation of alcohols under visible light irradiation for 4h. For comparison, the photoactivity yield over Pd/CeO₂-NPs and Pd/commercial CeO₂ is also shown.

Figure S4. Photoluminescence (PL) spectra of the samples of Pd/CeO₂-NPs, Pd/commercial CeO₂ and the bare support of commercial CeO₂ and CeO₂-NPs (excited at a wavelength of 370 nm).

Figure S5. Controlled experiments using different radicals scavengers: *tert*-butyl alcohol (TBA) for hydroxyl radicals; ammonium oxalate (AO) for holes; benzoquinone (BQ) for superoxide radicals, and AgNO₃ for electrons, for oxidation of cinnamyl alcohol in water over Pd/CeO₂-NPs under visible light irradiation for 4 h.

Figure S6. Controlled experiments using different radicals scavengers: *tert*-butyl alcohol (TBA) for hydroxyl radicals; ammonium oxalate (AO) for holes; benzoquinone (BQ) for superoxide radicals, and AgNO₃ for electrons, for oxidation of n-hexanol in water over Pd/CeO₂-NPs under visible light irradiation for 4 h.

Figure S7. The electron spin resonance (ESR) spectra of superoxide radicals and hydroxyl radicals trapped by DMPO over the suspensions of Pd/CeO₂-NPs and Pd/commercial CeO₂ under visible light irradiation.

Figure S8. Time-dependent •OH-trapping fluorescence spectra (excited at a wavelength of 312 nm) by the reaction of terephthalic acid (TA) with the •OH radicals photogenerated by the Pd/CeO₂-NPs photocatalyst in an aqueous phase under visible light irradiation.

Table S1. Selective oxidation of various alcohols in organic solvent of benzonitrile (BTF) over Pd/CeO₂-NPs and Pd/commercial CeO₂ under visible light irradiation (λ > 420 nm) for 4 h at room temperature.^a

Figure S9. The nitrogen adsorption-desorption isotherms of the samples of Pd/CeO₂-NPs and

Pd/commercial CeO₂; below is the summary of surface area, total pore volume and pore size of Pd/CeO₂-NPs and Pd/commercial CeO₂.

Figure S10. Bar plot showing the adsorption capacity of Pd/CeO₂-NPs and Pd/commercial CeO₂ toward substrate alcohols after the adsorption-desorption equilibrium is reached in the dark.

Appendix for samples photographs.

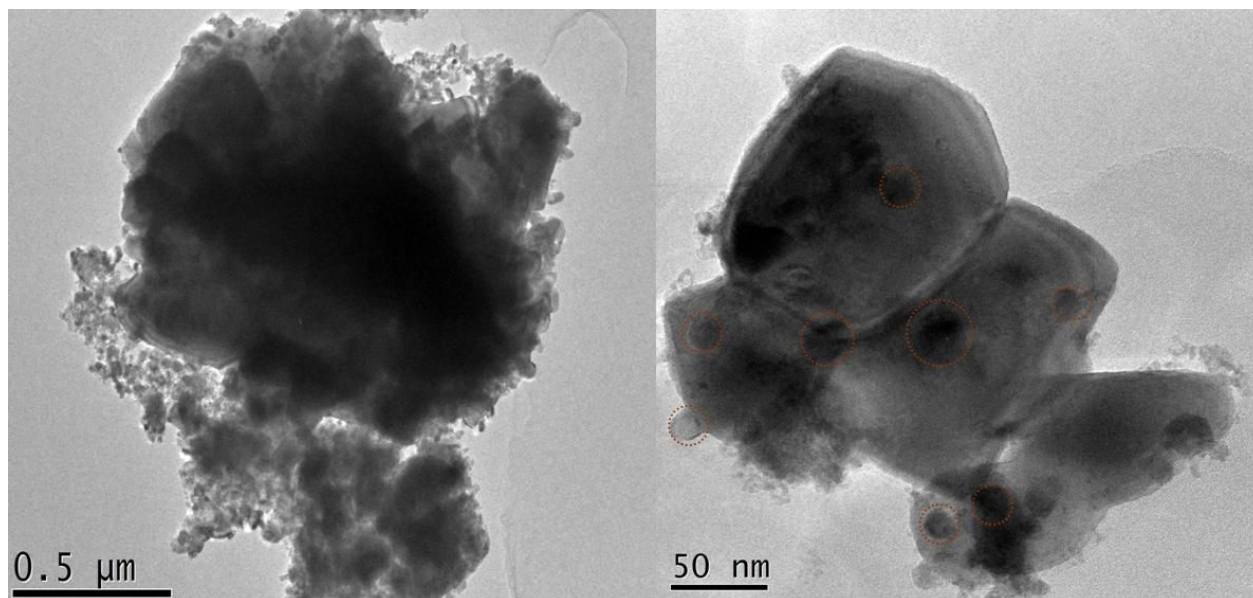


Figure S1. Typical TEM images of Pd/commercial CeO₂.

Note: Red circled area is the Pd particles supported on commercial CeO₂. It is clear to observe the obvious aggregation of Pd particles as compared to the original Pd colloidal nanoparticles.

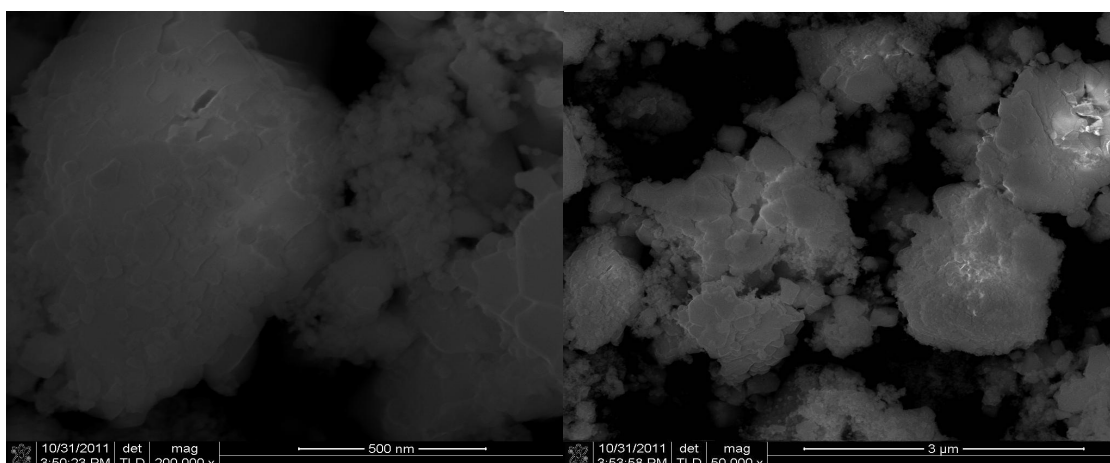


Figure S2. Typical SEM image of Pd/commercial CeO₂ at different magnification.

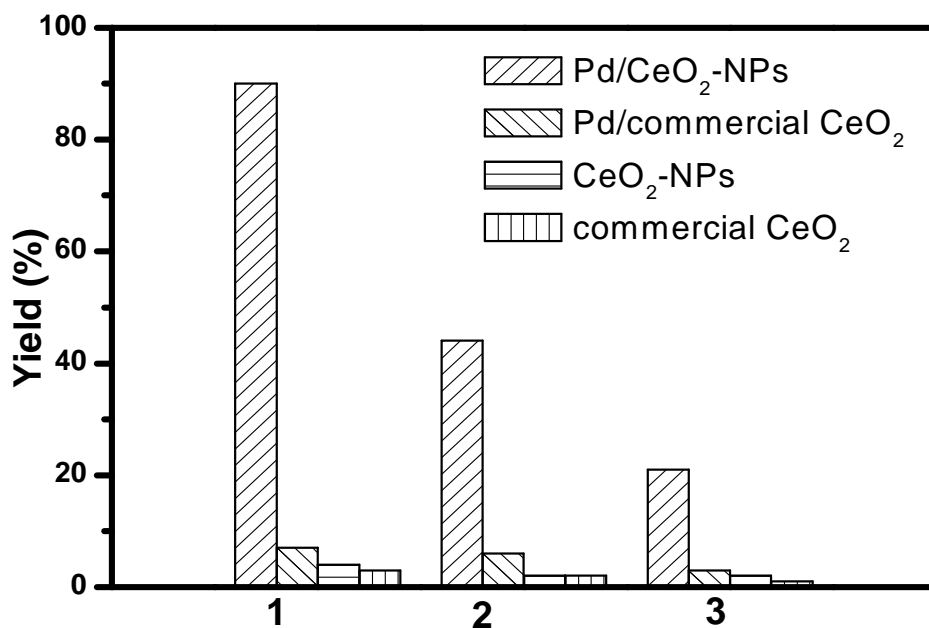


Figure S3. Controlled experiments using the bare CeO₂ nanoparticles (CeO₂-NPs) and commercial CeO₂ for oxidation of alcohols under visible light irradiation for 4h. For comparison, the photoactivity yield over Pd/CeO₂-NPs and Pd/commercial CeO₂ is also shown.

Note: number 1: benzyl alcohol; 2: cinnamyl alcohol; 3: n-hexanol.

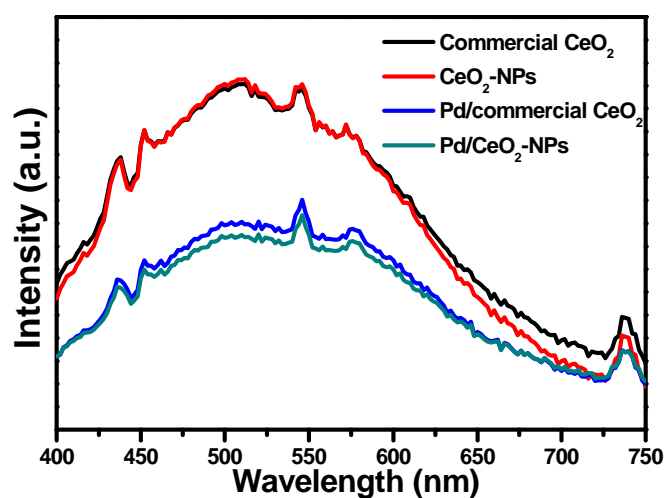


Figure S4. Photoluminescence (PL) spectra of the samples of Pd/CeO₂-NPs, Pd/commercial CeO₂ and the bare support of commercial CeO₂ and CeO₂-NPs (with an excitation wavelength of 370 nm).

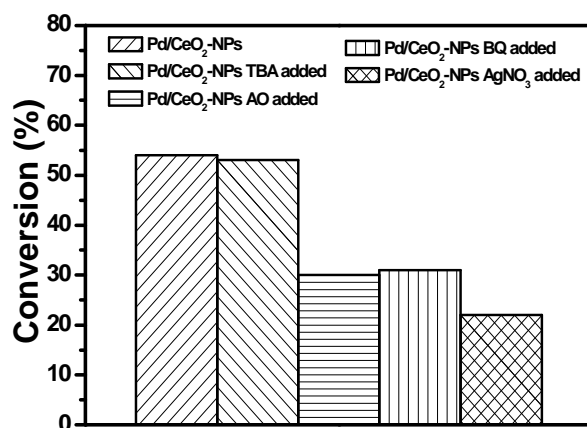


Figure S5. Controlled experiments using different radicals scavengers: *tert*-butyl alcohol (TBA) for hydroxyl radicals; ammonium oxalate (AO) for holes; benzoquinone (BQ) for superoxide radicals, and AgNO₃ for electrons, for oxidation of cinnamyl alcohol in water over Pd/CeO₂-NPs under visible light irradiation for 4 h.

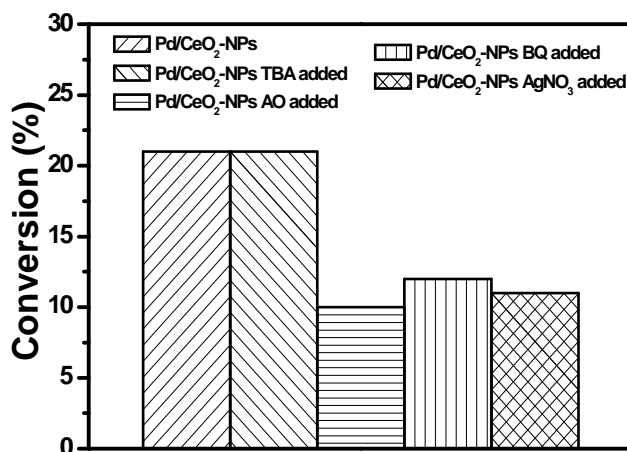


Figure S6. Controlled experiments using different radicals scavengers: *tert*-butyl alcohol (TBA) for hydroxyl radicals; ammonium oxalate (AO) for holes; benzoquinone (BQ) for superoxide radicals, and AgNO₃ for electrons, for oxidation of n-hexanol in water over Pd/CeO₂-NPs under visible light irradiation for 4 h.

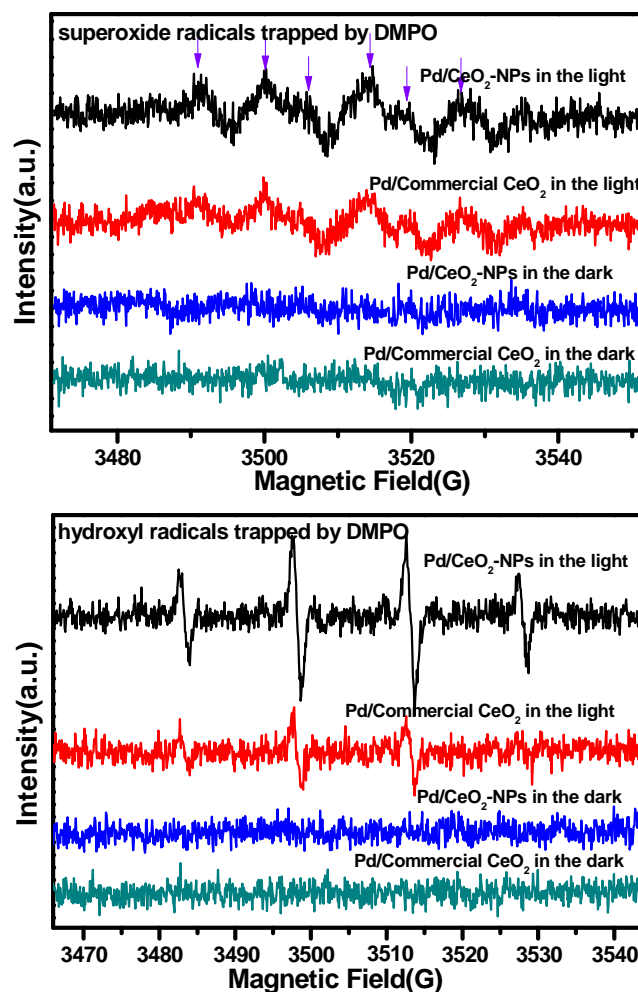


Figure S7. The electron spin resonance (ESR) spectra of superoxide radicals and hydroxyl radicals trapped by DMPO over the suspensions of Pd/CeO₂-NPs and Pd/commercial CeO₂ under visible light irradiation.

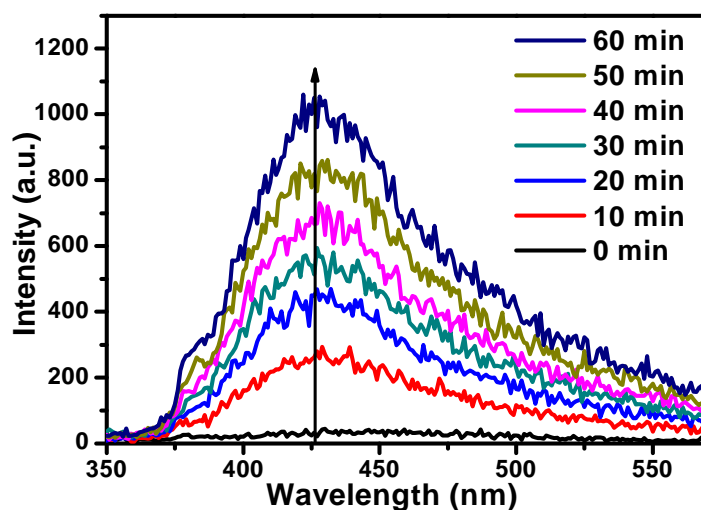
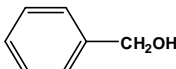
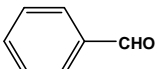
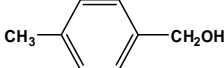
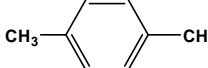
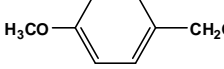
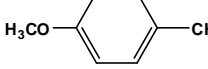
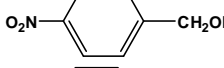
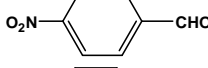
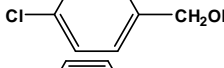
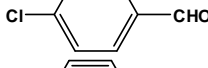
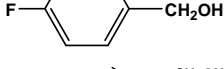
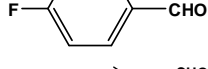
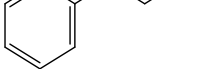

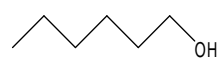
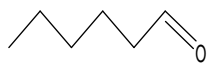




Figure S8. Time-dependent •OH-trapping fluorescence spectra (with an excitation wavelength of 312 nm) by the reaction of terephthalic acid (TA) with the •OH radicals photogenerated by the Pd/CeO₂-NPs photocatalyst in an aqueous phase under visible light irradiation.

Table S1. Selective oxidation of various alcohols in organic solvent of benzotrifluoride (BTF) over Pd/CeO₂-NPs and Pd/commercial CeO₂ under visible light irradiation ($\lambda > 420$ nm) for 4 h at room temperature.^a

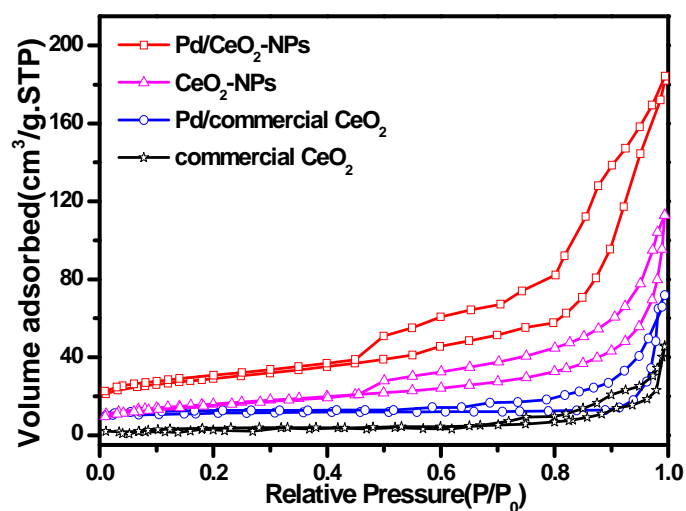
Entry	Substrate	Product	Conv.(%)	Sel.(%)
1			99 (4)	100 (100)
2			51 (3)	100 (100)
3			49 (3)	100 (100)
4			58 (2)	100 (100)
5			47 (3)	100 (100)
6			51 (4)	92 (92)
7			41 (3)	84 (84)
8			19 (1)	100 (100)
9			18 (1)	100 (100)

^a The data in parenthesis are conversion and selectivity over Pd/commercial CeO₂ under identical reaction conditions.

Note: The high selectivity to target products, aldehydes, as obtained in the solvent of water over Pd/CeO₂-NPs and Pd/commercial CeO₂ under visible light irradiation is similar to that as obtained in the solvent of benzotrifluoride (BTF) in which no hydroxyl radicals are generated.^{S1,S2} This strongly suggests that, for the highly active visible light Pd/CeO₂-NPs photocatalyst, the presence of hydroxyl radicals in water does not affect the selectivity in a considerable way.

Ref. S1: Zhang, M.; Chen, C.; Ma, W.; Zhao, J. Visible-Light-Induced Aerobic Oxidation of Alcohols in a Coupled Photocatalytic System of Dye-Sensitized TiO₂ and TEMPO. *Angew. Chem. Int. Ed.* **2008**, *47*, 9730-9733.

Ref. S2: Zhang, Y.; Tang, Z. R.; Fu, X.; Xu, Y. J. Engineering the Unique 2D Mat of Graphene to Achieve Graphene-TiO₂ Nanocomposite for Photocatalytic Selective Transformation: What Advantage does Graphene Have over Its Forebear Carbon Nanotube? *ACS Nano* **2011**, *5*, 7426-7435.



Sample	Pd/CeO ₂ -NPs	CeO ₂ -NPs	Pd/ commercial CeO ₂	commercial CeO ₂
Surface area (m ² /g)	145	56	24	3
Pore volume (cm ³ /g)	0.36	0.17	0.11	0.03

Figure S9. The nitrogen adsorption-desorption isotherms of the samples of Pd/CeO₂-NPs and Pd/commercial CeO₂; below is the summary of surface area and total pore volume of Pd/CeO₂-NPs and Pd/commercial CeO₂.

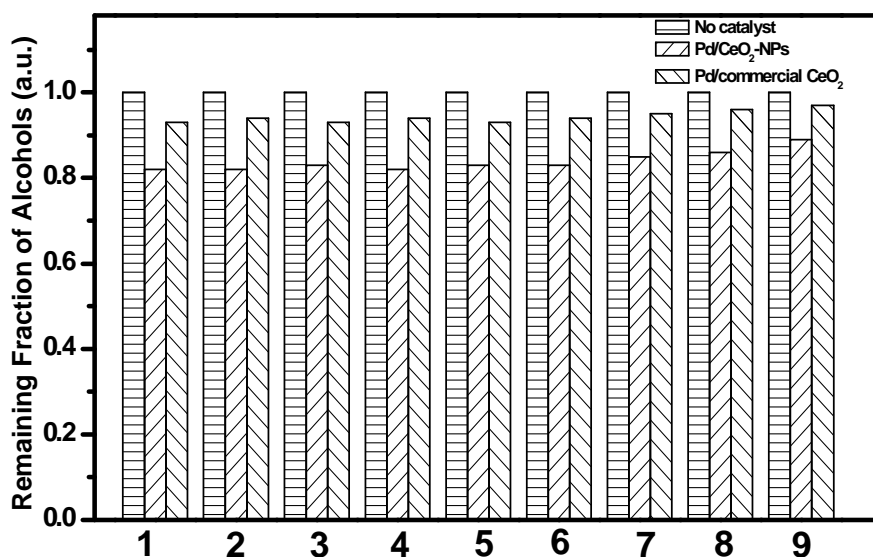


Figure S10. Bar plot showing the adsorption capacity of Pd/CeO₂-NPs and Pd/commercial CeO₂ toward substrate alcohols after the adsorption-desorption equilibrium is reached in the dark.

Note: numbers 1-9 represent the same substrate alcohols as entry in **Table S1**.

Note: It is clear from **Figure S10** that the adsorption capacity of Pd/CeO₂-NPs is higher than Pd/commercial CeO₂ toward substrate alcohols, which is in line with the higher surface area and pore volume of Pd/CeO₂-NPs than Pd/commercial CeO₂.

Appendix for samples photographs.

